Insurance Institute for Business & Home Safety

Where building science leads to real-world solutions.

Comparison of Field and Full-Scale Laboratory Peak Pressures at the IBHS Research Center

Results Obtained from Full-Scale Wind Tunnel Tests

The validation of the IBHS Research Center's ability to reproduce flow field characteristics and the pressure on the surface of a building, compared to both full-scale and model-scale wind tunnel results.

Murray J. Morrison [1], Tanya M. Brown [2], Zhuzhao Liu[3]

[1]*Insurance Institute for Business & Home Safety, 5335 Richburg Rd., Richburg, SC 29729; PH (803) 789-4218; email: mmorrison@ibhs.org*
[2]*Insurance Institute for Business & Home Safety, 5335 Richburg Rd., Richburg, SC 29729; PH 803-789-4208; email: tbrown@ibhs.org*
[3]*Insurance Institute for Business & Home Safety, 5335 Richburg Rd., Richburg, SC 29729; PH 803-789-4205; email: zliu@ibhs.org*

ABSTRACT

The Insurance Institute for Business & Home Safety (IBHS) Research Center is capable of subjecting full scale structures to high wind loads. In order to validate the facility, comparisons of the mean velocity, turbulence intensity profiles and turbulent spectra are made to both field measurements from Texas Tech University and theoretical profiles and spectral estimates. The match of the mean velocity profiles and turbulence intensity profiles was good in both the longitudinal and lateral directions. The match of the turbulent spectra from the IBHS facility is good, with a small spectra gap between wave numbers of 0.01 and 0.1 and too much energy at small scales, similar to model scale wind tunnels. The match of point pressures on a building compared to model scale and full scale experiments is good, with the results from the IBHS facility generally falling between the full scale and model scale results in the separated regions on the roof.

INTRODUCTION

Twenty years ago Hurricane Andrew made landfall in Florida causing significant damage estimated between $20-25 billion (USD) in Florida and an additional $1 billion (USD) in Louisiana (HUD, 1993). As a result of Hurricane Andrew, improvements were made to the South Florida Building Code and adopted in Broward and Miami Dade counties in 1994. Enhanced high-wind design and construction requirements were adopted in other Florida coastal counties in late 1995, and a state wide building code was adopted on March 1, 2002. Gurley et. al. (2006) have shown the newer homes built to this improved statewide standard suffered less damage than those built to the previous standard. Despite improvements made to building codes in Florida and other jurisdictions, annual losses due to hurricanes have been increasing dramatically due to an increase in population and infrastructure in hurricane-prone regions (Pielke et al., 2008). Consequently, there is a critical need to make further improvements to building codes and to develop cost effective mitigation strategies for existing buildings. A detailed understanding of component performance and how structural components and connections fail in high winds is an essential underpinning for these efforts.

Model scale wind tunnel studies provide excellent information on the actual wind loads that occur on buildings. However, relating these wind loads to specific structural failures can be a significant challenge. Some scale wind tunnel studies have used failure models (e.g. Visscher and Kopp, 2007) to predict the failure wind speed of certain structural components. However, these types of experiments have significant assumptions, for example the failure mode is assumed implicitly.

Moreover, the modeling of the structural details posses a significant challenge. In contrast, typical standardized product tests model the structural details exactly, with the exception of specimen boundary condition. However, these structural tests involve significant simplification of the wind loading usually applying static, slow increasing ramps or very basic cyclic loading.

In order to provide more realistic predictions of the performance of full scale structures under high winds the IBHS Research Center depicted in Figure 1 was constructed in 2010. The core facility at the research center is a large wind tunnel, which enables actual full-scale structures and components to be tested under realistic high wind conditions. This approach removes the modeling and scaling issues of the structural system found in model scale wind tunnel tests, while bringing increased realism to the wind loads compared to typical standard structural testing. The key challenge of the IBHS Research Center test chamber is the ability to properly generate the appropriate mean and turbulence intensity profiles, along with the correct power spectrum distribution of typical wind speed boundary layer winds. The following paper describes the validation of the IBHS Reach Center's ability to reproduce flow field characteristics and the pressure on the surface of a building, compared to both full-scale and model-scale wind tunnel results.

Figure 1 (Left) Aerial photograph of the newly-constructed IBHS Research Center in Richburg, South Carolina. (Right) Photograph of the 105 fans that generate the flow through the test chamber.

FACILITY DETAILS AND FLOW CONTROL ELEMENTS

The central element of the IBHS Research Center is a specially-designed open-jet wind tunnel which is large enough to subject full-scale one- or two-story residential structures and commercial buildings with flat or pitched roofs to a variety of wind conditions or the reproduction of specific wind events. The wind tunnel has an exceptionally large test chamber: 44.2 m (145’) wide by 44.2 m (145’) long, with a clear interior height of 18.3 m (60’). However, the test section is relatively short, and as a result cannot naturally produce the mean and turbulence characteristics of the atmospheric boundary layer (ABL). Instead to generate the correct mean and turbulence intensity profiles along with the correct turbulence characteristics the facility relies on both active and passive control elements, which are discussed in more detail below. The wind flow is produced by 105 1.68 m (5.5’) diameter vane-axial fans, shown in Figure 1, with 350 hp medium voltage electric motors. The 105 fan array is broken up into 15 cells, with 5 cells spanning horizontally and 3 cells vertically. The contraction from the fans to the inlet, shown in Figure 2, is approximately 2:1. The resulting inlet to the test chamber has dimensions of 19.8 m (65 ft) by 9.1 m (30 ft). Figure 3 provides a schematic of the overall layout of the test chamber. The fans in each cell can be controlled independently of each other, with the lower cells containing 9 fans each and the middle and upper cells containing 6 fans each. The speed of each fan cell is independently controlled by a programmable logic controller (PLC), which can update the running speed of the fans at a maximum frequency of 4 Hz, following a preset program of fan speeds designed to simulate the large scale flow characteristics of the ABL. The preset fan speed traces can be generated to mimic the mean and expected large scale turbulence of a generic boundary layer wind or can tailored to a specific field measured wind record from an actual event. At full power the fans have a running speed of approximately 1800 RPM and the entire fan array draws approximately 30 MW of power. Nominally the fans are able to accelerate up to a rate of 260 RPM/s, although this number is dependent upon a number of factors such as the actual speed of the fan and the size of the specimen within the test chamber. Two additional flow control elements, the directional wind vanes and spires, both shown in Figure 2, are used in conjunction with the fan speed variations to develop the appropriate flow characteristics to simulate the ABL. Similar to the fans; the wind vanes are active control elements and are controlled by the same PLC system as the fans. In total there are 16 wind vanes that extend the entire height of the inlet. The 16 wind vanes are broken into five groups which can be rotated independently of each other, between -15° to +15° with 0° being in the streamwise direction. The movement of the wind vanes produces large-scale flow fluctuations in the lateral direction. Each of the lower cells has 3 spires with a base diameter of 0.46 m (1.5 ft) and a height of 4.2 m (14 ft), resulting in an apex angle of 6°. Each of the middle cells also has 3 spires with a height of 1.2 m (approximately 50% of the cell height), with the same apex angle as the spires in the lower cells. In both the lower and middle cells the spires are equally spaced within each of the cells. In addition, to altering the mean flow profile within the lower and middle cells the spires are able to produce turbulence at higher frequencies than that produced by modulation of the fan speeds.

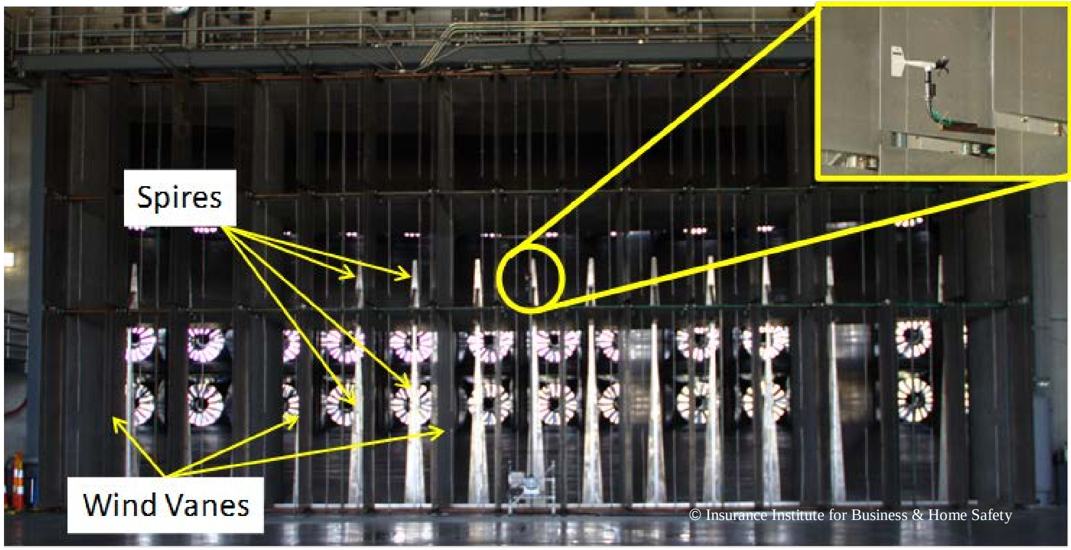

Figure 2 Identification of key flow control aspects of the IBHS Research Center test chamber.

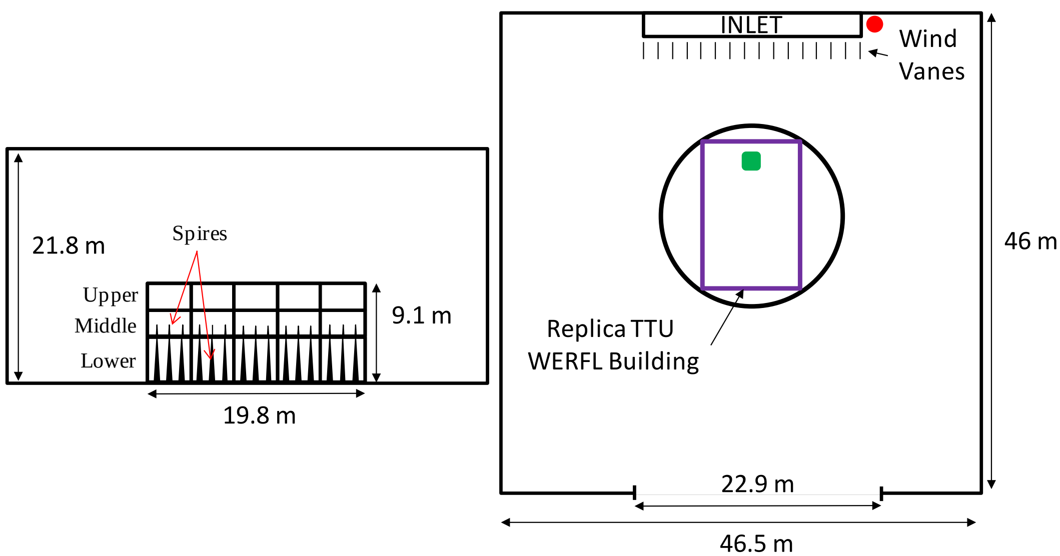

Figure 3 Layout of the IBHS Research Center test chamber and inlet from the fans.

EXPERIMENTAL SETUP

For the current series of experiments full scale benchmark data were obtained from the Wind Engineering Research Field Laboratory (WERFL) at Texas Tech University (TTU). The WERFL experimental building is a full-scale test building that has been used since 1989 to collect wind-induced pressure data in a natural, open exposure environment in Lubbock, Texas (Levitan and Mehta, 1992a, 1992b). The data from the WERFL site provide simultaneous wind flow measurements from a 48.8 m (160 ft) meteorological tower and surface pressures measurements from the WERFL building. The WERFL building has plan dimensions of 9.1m (30 ft) by 13.7 m (45 ft) with an eave height of 4.0 m (13 ft) and a roof slope of 0.25 on 12. For the flow field measurements the modulation of both the fan speeds and the rotation of the vanes are tailored to a single case obtained from the WERFL site. To assess the effect of the wind speed, a second case was created by doubling the velocity data from the WERFL site case. Each case was conducted both with and without the spires installed. The surface pressure experiments were conducted using the same 4 cases as the flow field measurements. Table 1 provides a summary of the test matrix for both the flow field and surface pressure measurements reported in the current paper. Brown et. al. (2011) provides additional details on the selection of the field data from TTU and the replica building constructed for testing at IBHS.

Table 1 List of test parameters for the current paper

Test Number	TTU WERFL Case #	Spires installed	Wind Direction To building
Case1	620	No	6°
Case2	620 (wind speed doubled)	No	6°
Case3	620	Yes	6°
Case4	620 (wind speed doubled)	Yes	6°

Flow Field Measurements

In order to assess the mean and turbulence characteristics of the flow field four cobra probes were mounted to an adjustable gantry system (shown in Figure 4) in both horizontal and vertical arrangements. Typical spacing between probes in both arrangements is 0.61 m (2 ft), and the height of the measurements was adjusted by raising and lowering the cross member on the gantry. The gantry was placed 11.6 m (38 ft) downstream of the inlet to the test chamber, with the vertical profile measurements located along the center line of the test chamber as indicated by the green square in Figure 3. Measurements were taken at 0.61 m (2 ft) intervals between 0.61 m and 7.3 m above the test chamber floor. The data collected in the IBHS Research Center's test chamber is compared to both TTU field data described above and to theoretical mean velocity and turbulence intensity profiles and target turbulence spectra from ESDU (1982).

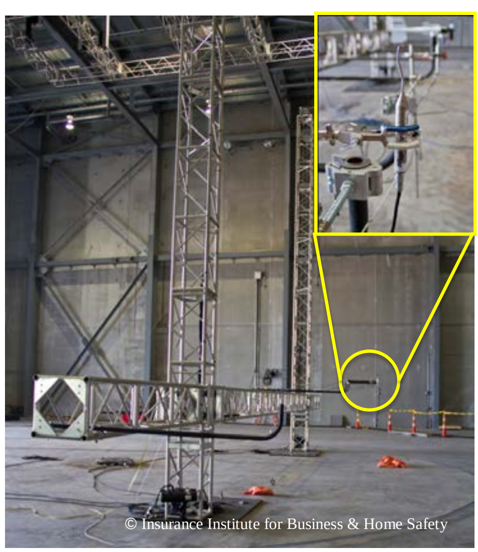

Figure 4 Photograph of the gantry and cobra probes in a horizontal configuration.

Surface Pressure Measurements

In order to validate the ability of the IBHS wind test facility to produce realistic wind pressures on test buildings, a replica of the TTU WERFL experimental building was constructed and tested at the IBHS Research Center. Pressure taps were installed on the IBHS replica building in the same 204 locations as the original building (at TTU), as found in Lombardo (2009). The location of the building within the IBHS test chamber is shown in Figure 3 and is 7.9 m (26 ft) or two times the building height downstream of the wind vanes. The surface pressure data were acquired at 100Hz and low pass filtered to 15Hz to be consistent with the full scale field measurements from TTU. The surface pressure data were then converted to non-dimensional pressure coefficients Cp using:

$$Cp = \frac{P - P_\infty}{0.5\rho V^2} \quad (1)$$

where P is the surface pressure, P_∞ is the static pressure within the test chamber and V is the 15 minute mean velocity at roof height. The location of the static pressure, P_∞, for the current set of experiments is shown by the red circle in Figure 3. This location was chosen as the optimal location for the static pressure reference through a series of experiments (not presented here) where the pressure at multiple points throughout the test chamber were measured. Ideally the static pressure reference location needs to capture the changing pressure within the test chamber due to the varying of the fan speeds, but not be influenced by the flow within the test chamber. The roof height velocity, V, is obtained from an RM Young anemometer at roof height at the inlet to the test chamber as shown in Figure 2. The surface pressures obtained from the IBHS test chamber are compared to the field measurements from the TTU WERFL data described above. In addition model scale wind tunnel data of the WERFL building, obtained from the University of Western Ontario, is also used for comparison, details of the model scale wind tunnel experiments can be found in Ho et. al. (2005).

RESULTS

Flow Field

Figure 5 and Figure 6 present the mean wind velocity profile and the longitudinal (*Iu*), lateral (*Iv*) and vertical turbulence (*Iw*) intensity profiles for the four cases outlined in Table 1. Overall, the match between the IBHS mean velocity profile when the spires are present (light and dark blue cases) to the target field cases (red) and the ESDU (1982) theoretical profile (black) is good. A slight deficit in the mean profile exists at the interface between the lower and middle cells. The match of the longitudinal turbulence intensities is good, with a slight deviation in the upper parts of the middle cell and lower part of the upper cell where no spires are present. The IBHS lateral turbulence intensities show more scatter than the longitudinal turbulence intensities as compared to the ESDU profile, however, overall the scatter seems to follow the ESDU profile and is lower than the lateral turbulence intensity of the TTU field data. The match of the vertical turbulence intensity profile for the field data case and all of the IBHS cases to the theoretical ESDU profile is relatively poor. In the case of the field data, the poor match is likely the result of instrument resolution since the velocities in the vertical direction are relatively small as compared to the longitudinal and lateral directions. The IBHS facility has no active mechanism to control the turbulence in the vertical direction, although the spires appear to provide an increase in *Iw* over the no spire cases. In all profiles the collapse of the two different wind speed cases conducted in the IBHS test chamber is quite good with the largest deviations occurring in the mean and *Iu* profiles. However, these quantities are the ones most affected by the modulation of the fan speeds and since tests are conducted on different days under different external meteorological conditions, this may be the natural variability of the flow within the test chamber. Further, long-term experiments are currently planned to assess the sensitively of the flow within the test chamber to external atmospheric conditions. It is expected that the external meteorological conditions may be less significant when higher mean wind speeds are being simulated within the test chamber, since ambient wind speed will represent a lower percentage of the wind speed within the test chamber.

It should be noted that a portion of the turbulence within the test chamber is being generated through the use of active control elements and the fetch is relatively short, there is not enough distance for the turbulence cascade to fully establish itself. Consequently, it is possible that while the turbulence intensities have the correct magnitude, the scales of turbulence may not match as well as would be desired. The next section examines the scales of turbulence in more detail.

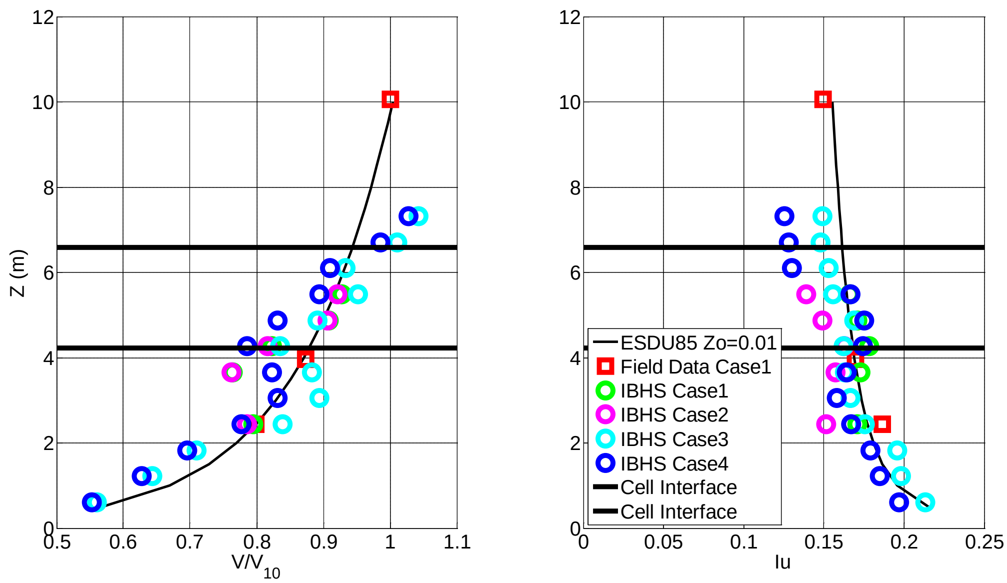

Figure 5 Mean velocity (left) and longitudinal turbulence intensity (*Iu*) (right) profiles.

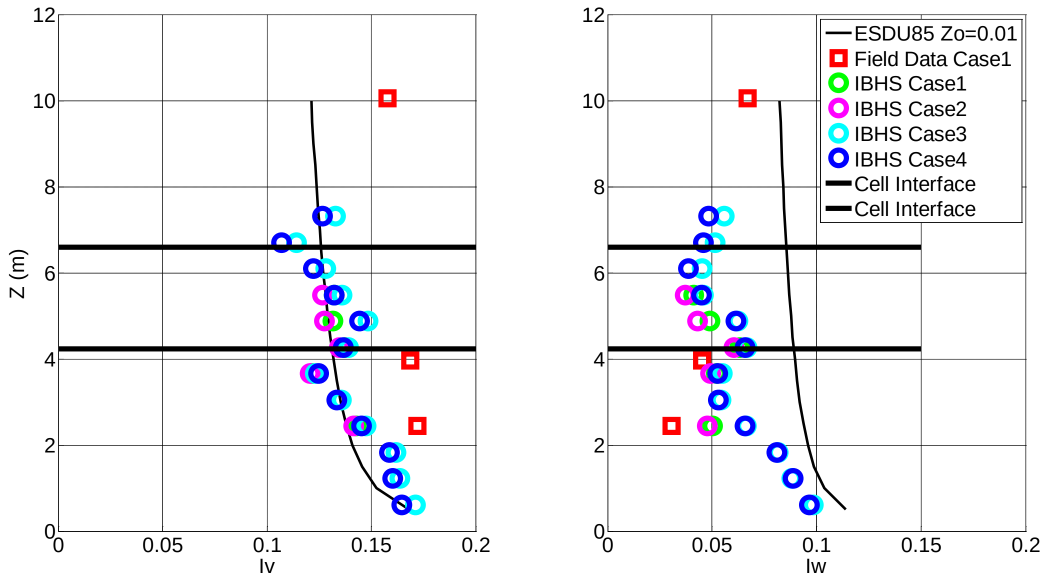

Figure 6 Lateral (*Iv*) (left) and vertical (*Iw*) (right) turbulence intensity profiles.

Since the active control elements within the IBHS test chamber can artificially change the standard deviation of the velocity fluctuations, if too much energy is added at lower frequencies (large turbulent scales) using both the fans and the wind vanes, normalizing the standard deviation squared, which is common for wind spectra comparison may skew the comparison of the power spectra. As a result the power spectra presented herein are normalized by the mean velocity squared, similar to Davenport (1961). Figure 7 to Figure 9 present the longitudinal, lateral and vertical power spectra respectively for the four cases presented in Table 1. Also, to aid in the comparison, the generalized spectral models from ESDU (1985), Kaimal et. al. (1972) and Simiu and Scanlan (1996), are included in Figure 7 through Figure 9. The purpose of showing multiple generalized spectra is to provide a basis of comparison for the current results and not to discuss the differences in the generalized spectra themselves. Mann (1998) provides a detailed discussion of the various spectral models of the ABL. As discussed by Mann (1998) the ESDU equations do not follow the surface layer scaling. The ESDU spectra provided in Figure 7 to Figure 8 are calculated based on the mean velocities of Cases 1 and 3.

The match of the longitudinal spectra in Figure 7 between the two field cases and ESDU is quite good up to a wave number (F/V) of 0.1 which corresponds to a Frequency of approximately 1 Hz for Cases 1 and 3 and 2 Hz for Cases 2 and 4. This drop off of the field spectra is a result of the frequency response of the field instrumentation. By comparing with spires to without spire cases from the IBHS test chamber, the effect of the spires is apparent at wave numbers greater than approximately 0.03. At wave numbers less than 0.03 the spectra of with and without spire cases match closely, however, there is a significant shift in the spectra between the low and high velocity cases. This indicates that at these lower wave numbers the turbulent spectra is dominated by the fan and vane modulation which, unlike the turbulence generated by the spires, do not scale with wind velocity. This is likely a limitation of the physical frequency response of the fans and vanes being able to modulate the inlet flow conditions. Comparing IBHS Case 1 and 3 to the field and ESDU spectrum, the match up to a wave number of 0.01 is good. Between wave numbers of 0.01 and 0.1 the IBHS data shows a spectral gap where there is too little energy at these frequencies. As shown, the spires do help in adding energy at these frequencies, but are unable to fill this gap completely. At wave numbers greater than 0.1 the match is good, although the presence of the spires increases the amount of energy at smaller scales (as would be expected), creating too much fine-scale turbulence compared to the ESDU spectrum. The problem of too much fine scale turbulence is quite common in model scale wind tunnel experiments, (Tieleman, 2003 and Kopp et. al., 2005 for a discussion). However, unlike model scale wind tunnel facilities, the IBHS test chamber is able to match the large turbulent scales.

The lateral spectrum as shown in Figure 8 indicates similar trends to the longitudinal spectra, with a spectral gap as compared to the ESDU spectra between wave numbers of 0.01 and 0.3. However, the match to the TTU field data, which was the target, is quite good up to the frequency response cutoff of the field instrumentation. The effect of the spires can be observed at wave numbers greater than 0.1 and seem to scale reasonably well with wind speed. Similar to the longitudinal spectrum the turbulence generated at lower frequencies do not appear to scale with the wind speed. The match of the vertical spectrum in all experimental cases (field and IBHS facility) to the generalized spectrum models, shown in Figure 9, is not good. For the field data case this is likely a constraint of the instrumentation, since the wind speeds in the direction are fairly low. In the IBHS cases, there are no active mechanisms to generate turbulence in the vertical direction, making the match of the vertical spectrum difficult with such a short flow development length, although the spires do appear to have some effect at wave numbers greater than 0.1.

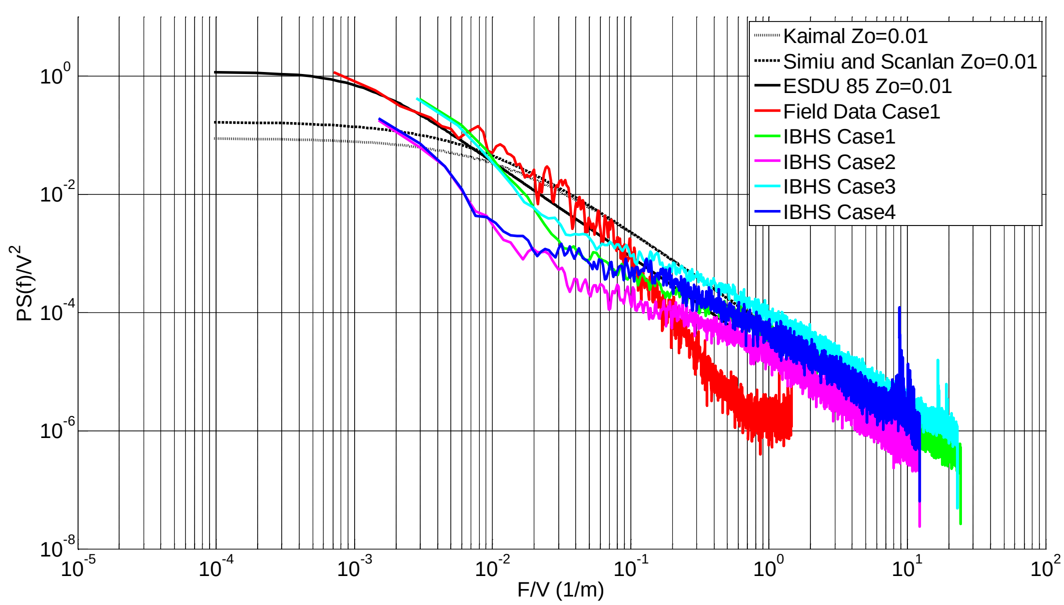

Figure 7 Longitudinal Power Spectrum (PS_U).

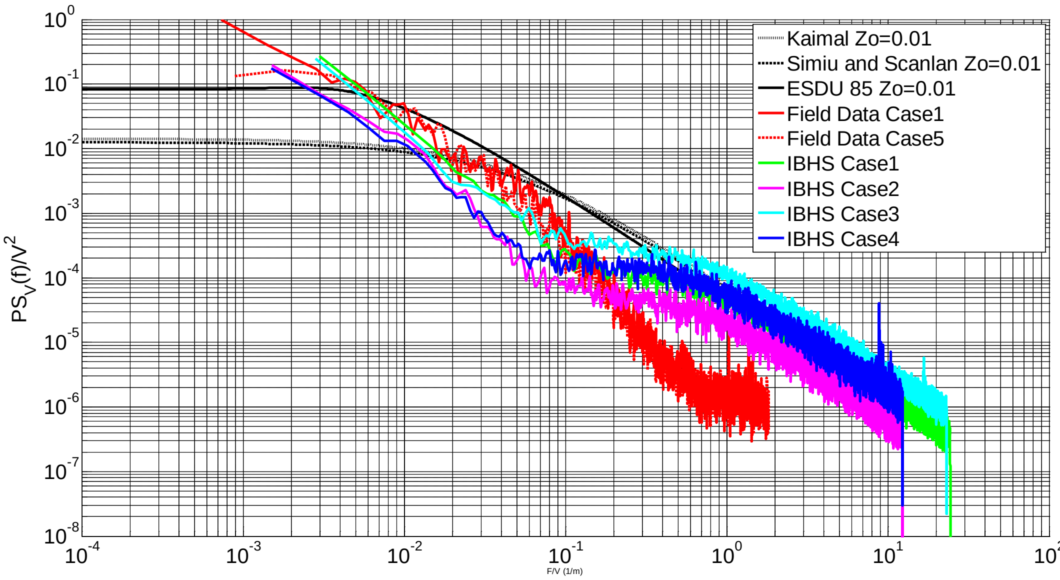

Figure 8 Lateral (PS_V) Power Spectrum.

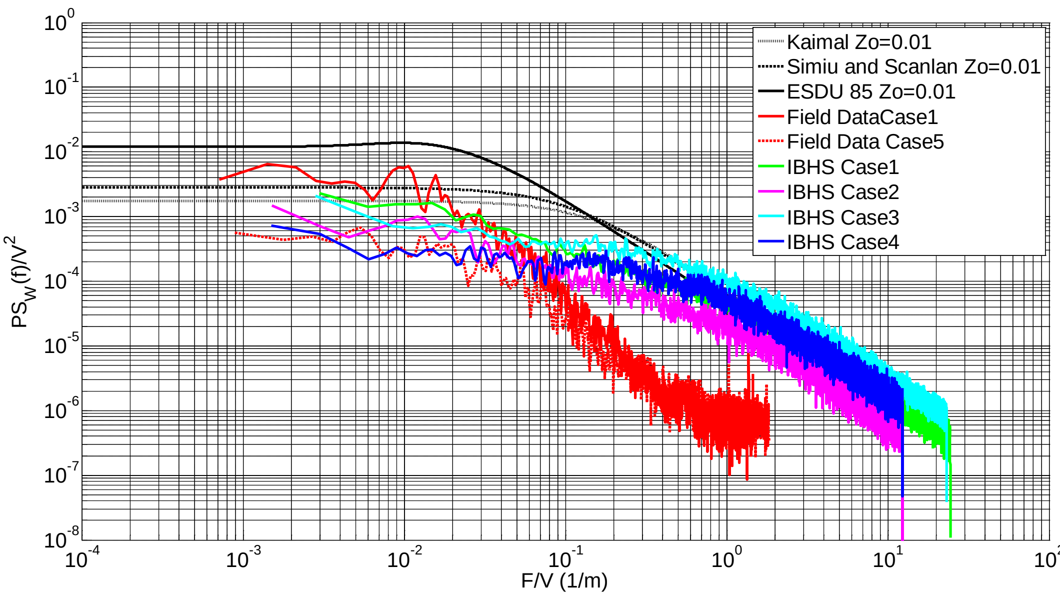

Figure 9 Vertical (PS_W) Power Spectrum.

Pressures

Figure 9 presents the mean pressure coefficients from a ring of pressure tap locations along the centerline of the building for Cases 1, 3 and 4 along with corresponding model scale wind tunnel data, from Ho et. al. (2005) and data from several model and full scale cases where cubes were tested in both uniform and boundary layer flows (Castro and Robins, 1977; Richards et. al., 2001). The importance of the wind spires is clearly shown in this plot. The surface pressures determined for the flow without wind spires (IBHS Case 1) matches very closely with results from Castro and Robins (1997) on a cube in uniform low turbulence flow, which is not typical of the ABL. In contrast, the results for cases with the wind spires match fairly well with the field and model scale wind tunnel studies along with the turbulent boundary layer results on a cube presented by Castro and Robins (1977). IBHS Cases 3 and 4 collapses almost perfectly indicated the surface pressures scale appropriately with wind speed. Finally it should be noted that the mean pressure coefficients for Cases 3 and 4 become positive in the field of the roof, which point to a possible static pressure bias in the IBHS cases. Moreover, the mean pressures in the center of the windward wall of the IBHS cases exceed those from the TTU field measurements and the model scale WERFL building results, which could also point to an incorrect static pressure reference, or incorrect dynamic pressure referencing. Further experiments are currently underway to examine both the static and dynamic pressure referencing issues within the IBHS test chamber.

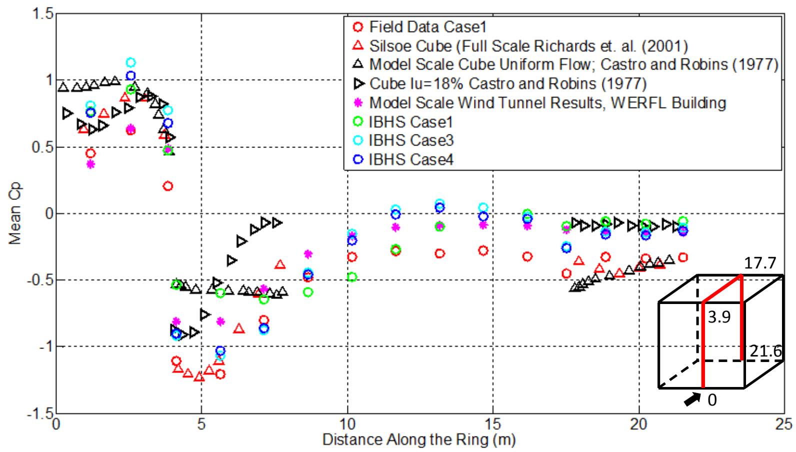

Figure 10 Comparison of IBHS test chamber results to benchmark studies on a ring around the centerline of the building. This ring is shown by the red line on the inset of the figure. The numbers on the figure corresponds to the distances provided on the x-axis of the figure, i.e. ground to the windward wall (0), windward wall to roof (3.9 m), roof to leeward wall (3.9 m to 17.7 m) and leeward wall to ground (17.7 m to 21.6 m).

Figure 10 through Figure 12 present the mean, standard deviation and minimum surface pressures, respectively for IBHS Case 4, Field Data Case 1 and model scale wind tunnel data of the WERFL building. It should be noted that the model scale wind tunnel results shown are at a wind angle of 10° rather than 6°, since this was the closest wind angle available from this database. Overall the match of mean and minimum surface pressures from the IBHS test chamber is quite good with values lying approximately in between the two benchmark studies, with the model scale wind tunnel results being slightly lower and the field results being slightly higher. However, the reattachment point for the IBHS data is further downstream than both the model scale wind tunnel and field data. Moreover, the standard deviations match reasonably well with the benchmark studies along the edges of the roof (in the separation regions of the roof) but have much higher values in the field of the roof after the reattachment point than both the benchmark studies. The longer reattachment length and higher standard deviation in the field of the roof may be a consequence of the spectral gap between wave numbers of 0.01 and 0.1. However, additional experiments and analysis will be required to determine the precise effect, if any; the spectral gap has on the surface pressures

Figure 13 shows the correlation coefficient calculated for each pressure tap location as compared to a pressure tap on the centerline of the building in the long dimension at 1.5 m (4.92 ft) from the windward edge. On the roof of the building, the IBHS Case 4 data and model scale wind tunnel data match well, while the TTU field data has a much higher correlation over the field of the roof. The correlation on the windward wall of both the TTU field data and the model scale wind tunnel data is highly inversely correlated (high negative value), while the IBHS data have a much lower (although still negative) correlation value. Since the pressures on the windward wall generally trend to be correlated with the temporally- changing wind speeds, this result suggests that the peak minimum pressures on the roof of the building are less correlated to the peak wind gust in the IBHS data as compared to both the model scale wind tunnel results and the full scale field measurements. However, these are simple correlation coefficients that average results over all frequencies and more insight may be gained by investigating coherence functions between pressure taps at various locations.

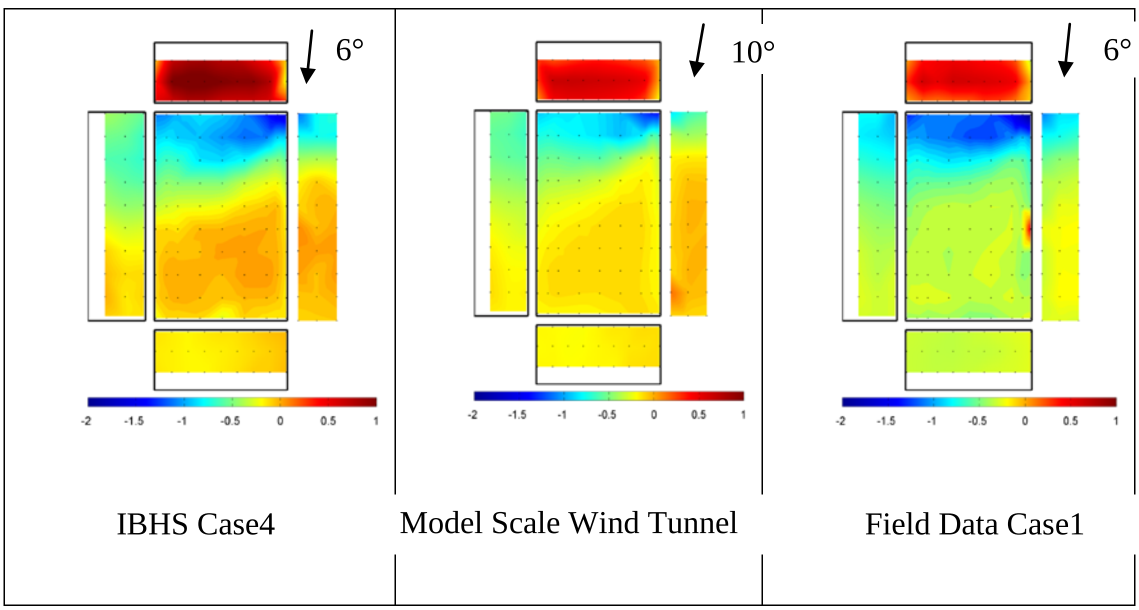

Figure 11 Comparison of mean surface pressure coefficients at a wind angle of approximately 6°.

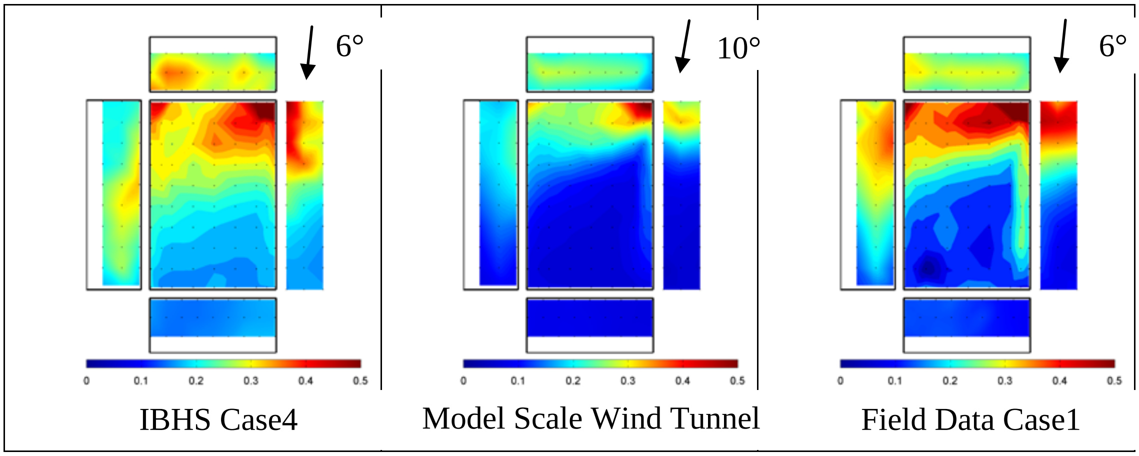

Figure 12 Comparison of standard deviation surface pressure coefficients at a wind angle of approximately 6°.

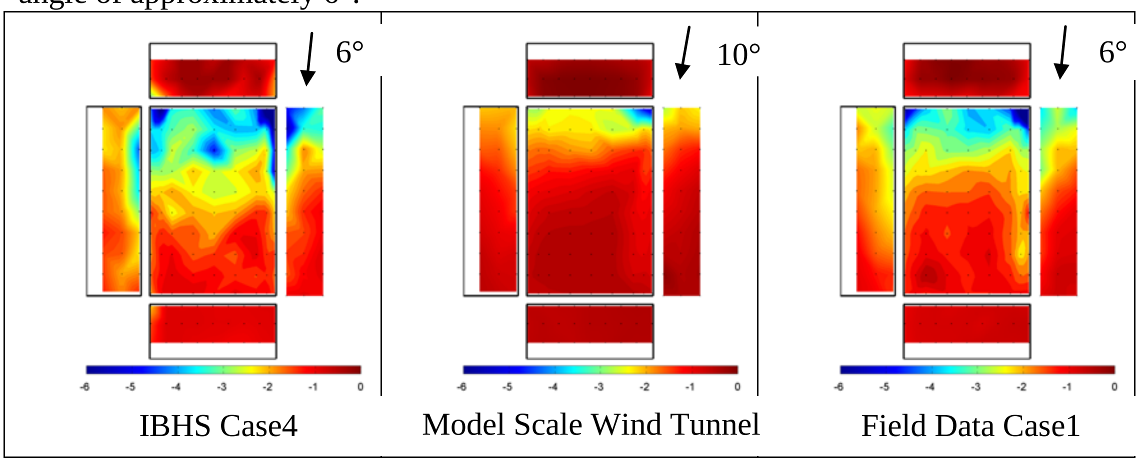

Figure 13 Comparison of minimum surface pressure coefficients at a wind angle of approximately 6°.

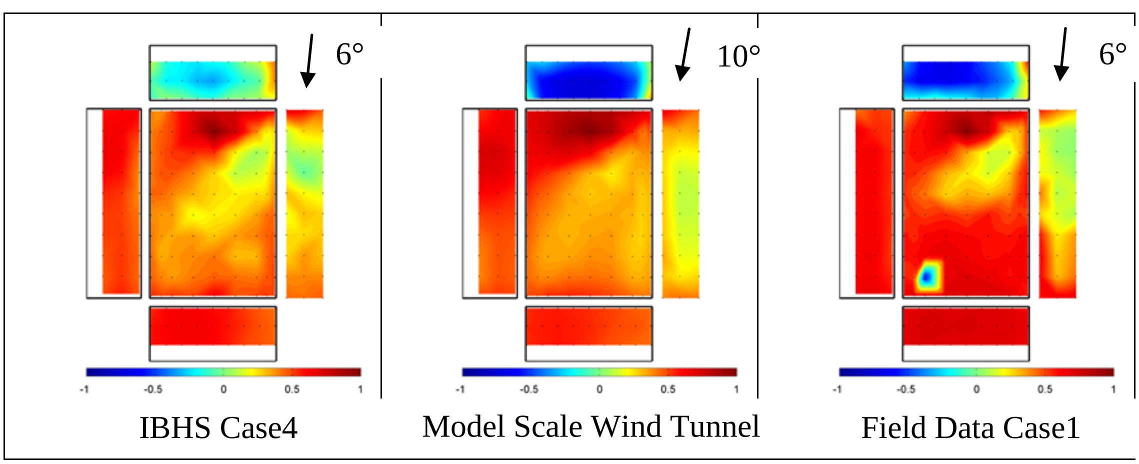

Figure 14 Comparison of the correlation contours at a wind angle of approximately 6°.

In addition, to the point pressure comparisons shown in Figure 9 through Figure 13, a comparison of mean area average coefficients on the roof of the building is presented in Figure 14. The area averages were calculated based on strips across the short dimension of the roof. These strips began with a width of 0.3 m (1ft), beginning at the windward edge of the roof and were increased by 0.3 m (1ft) increments to a maximum strip width of 9.1 m (30 ft). In addition, the area averages were also calculated for the entire roof (width of 13.7 m, 45 ft). Since, as previously discussed there may be a static referencing bias between the different studies the data was statically shifted so that the global mean roof uplift coefficient matched for all 4 cases and is shown in the inset of Figure 14. Even with the static correction applied to the data the model scale wind tunnel data has a lower mean coefficient at smaller areas in the separated regions of the roof. As the average area increases and encompasses more of the roof beyond the reattachment point the difference between the field and model scale wind tunnel results reduces with increasing area. The statically corrected mean area average results from the IBHS test chamber exceed those from the field data in the separated region of the roof, as a result of this shift. Due to the longer reattachment length the difference between the field data and the IBHS cases increases over the separated region of the roof, once the flow attaches the mean pressure coefficient reduces nearly linearly at a higher rate than the field or model scale wind tunnel measurements.

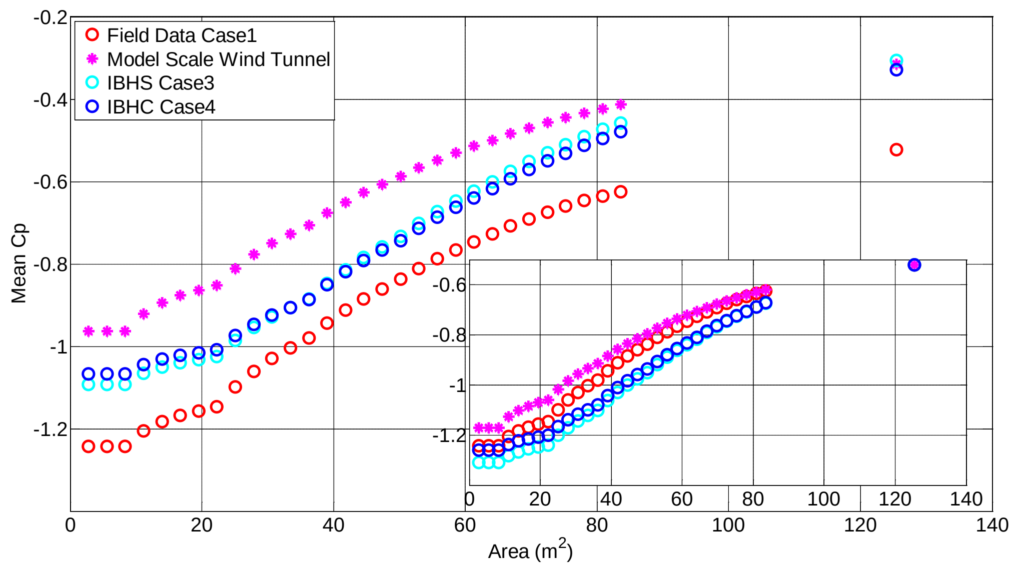

Figure 15 Comparison of mean area average pressure coefficients.

CONCLUSIONS AND FUTURE WORK

The simulation of the mean velocity profile longitudinal and lateral turbulence intensity profiles is good as compared with both field measurements and theoretical profiles from ESDU (1985). The longitudinal turbulence spectra of the IBHS test chamber shows a spectral gap between wave numbers of 0.01 and 0.1 and shows that the spires help to add energy at wave number greater 0.03. Similar to studies in model scale boundary layer wind tunnels the IBHS test chamber has too much energy and smaller turbulent scales when the spires are present as compared to the generalized spectrum. The comparison of surface pressures between the IBHS test chamber, full scale field data and model scale wind tunnel results is good with the point pressures generally falling between the model scale and full scale field measurements, based on the current reference pressure location, and method for determining the dynamic pressure. From the current results it appears that the static pressure may be biased high. Further, analysis of the present data is underway to examine the match of area average pressure coefficients of the IBHS test chamber data to the benchmark studies.

Currently, several projects are underway to further validate and understand the flow field within the IBHS test chamber, specifically, the variability of the flow within the test chamber based on external meteorological conditions. In addition, further experiments are planned to ensure proper static and dynamic pressure referencing of pressure coefficients.

REFERENCES

Brown, T.M., Liu, Z., Morrison, M.J., Cope, A.D., Smith, D.A., (2011). "Comparison of Field and Full-Scale Laboratory Pressure Data at the IBHS Research Center." *Proceedings of the 13th International Conference on Wind Engineering*, Amsterdam, Netherlands.

Castro, I.P., Robins, A.G. (1977). "The flow around a surface-mounted cube in uniform and turbulent streams." *Journal of Fluid Mechanics*, 79, 307-335.

Davenport, A.G., (1961). "The spectrum of horizontal gustiness near the ground in high winds." *Quarterly journal of the royal meteorological society*, 87, 194-211.

Department of Housing and Urban Development (HUD). (1993). *Assessment of Damage to Single- Family Homes Caused by Hurricanes Andrew and Iniki.* U.S., Office of Policy and Development and Research, HUD-0006262.

Engineering Science Data Unit (ESDU). (1982). Strong *winds in the atmosphere boundary layer. Part 1: mean-hourly wind speeds.* Data Item 82026, ESDU International Ltd.

Engineering Science Data Unit (ESDU). (1985). Characteristics *of atmospheric turbulence near the ground. Part II: single point data for strong winds (neutral atmosphere).* Data Item 85020, ESDU International Ltd.

Gurley, K.R., Masters, F.J. (2011). "Post 2004 hurricane field survey of residential building performance." *Natural Hazards Review,* 12(4), 177-183.

Ho, T.C.E., Surry, D., Morrish, D., Kopp, G.A. (2005). "The UWO contribution to the NIST aerodynamic database for wind loads on low buildings: Part1. Archiving format and basic aerodynamic data." *Journal of Wind Engineering and Industrial Aerodynamics,* 93, 1-30.

Kaimal, J.C., Wyngaard, J.C., Izumi, Y., Coté, O.R, (1972). "Spectral characteristics of surface- layer turbulence" Quarterly Journal of the Royal Meteorological Society, 98, 563-598.

Kopp, G. A., Surry, D., and Mans, C. (2005). "Wind effects of parapets on low buildings. 1: Basic aerodynamics and local loads." *Journal of Wind Engineering and Industrial Aerodynamics*, 93(11), 817–841.

Levitan M.L., Mehta K.C. (1992a). "Texas Tech field experiments for wind loads part I: meteorological instrumentation and terrain parameters" *Journal of Wind Engineering and Industrial Aerodynamics*, 43, 1565-1576.

Levitan M.L., Mehta K.C., (1992b). "Texas Tech field experiments for wind loads part II: Building and pressure measuring system," *Journal of Wind Engineering and Industrial Aerodynamics*, 43, 1565-1576.

Lombardo F.T. (2009). "Analysis and Interpretation of Thunderstorm Wind Flow and its Effects on a Bluff Body." *PhD Dissertation*, Texas Tech University, Lubbock Texas.

Pielke, R.A. Jr., Gratz, J., Landsea, C.W., Collins, D., Saunders, M.A., Musulin, R. (2008). "Normalized Hurricane Damage in the United States: 1900-2005." *Natural Hazards Review*, 9, 29-42.

Mann, J. (1998). "Wind field simulation." *Probabilistic Engineering Mechanics*, 13(4), 269-282.

Richards, P.J., Hoxey, R.P., Short, L.J. (2001). "Wind pressures on a 6 m cube" *Journal of Wind Engineering and Industrial Aerodynamics*, 89, 1553-1564.

Simiu, E., Scanlan, R. H. (1996). *Wind Effects on Structures: Fundamentals and Applications to Design*, 3rd Ed. (New York: Wiley)

Tieleman, H.W. (2003). "Wind tunnel simulation of wind loading on low-rise structures: a review." *Journal of Wind Engineering and Industrial Aerodynamics*, 91, 1627-1649.

Visscher B.T., Kopp G.A., (2007). "Trajectories of roof sheathing panels under high winds." *Journal of Wind Engineering and Industrial Aerodynamics*, 95, 697-713.